

THE EXPERIMENTAL DETERMINATION OF THE
BENDING AND TORSIONAL STIFFNESS OF A
BEAM WITH ROTATIONALLY CONSTANT
MOMENT OF INERTIA WITH VARYING
AMOUNTS OF PERMANENT TWIST

JOHN WOOLSTON
AND
LEON H. LEUTZ

Must 21

Artisan Gold Lettering & Smith Bindery

593 - 15th Street

Oakland, Calif.

Glencourt 1-9827

DIRECTIONS FOR BINDING

BIND IN

(CIRCLE ONE)

BUCKRAM

COLOR NO. 8854

FABRIKOID

COLOR _____

LEATHER

COLOR _____

OTHER INSTRUCTIONS

Letter in gold.

Letter on the front cover:

THE EXPERIMENTAL DETERMINATION OF
THE BENDING AND TORSIONAL STIFFNESS
OF A BEAM WITH ROTATIONALLY CONSTANT
MOMENT OF INERTIA WITH VARYING
AMOUNTS OF PERMANENT TWIST

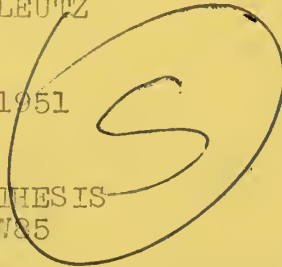
JOHN WOOLSTON
AND
LEON H. LEUTZ

^{shelf}
LETTERING ON BACK
TO BE EXACTLY AS
PRINTED HERE.

WOOLSTON
AND
LEUTZ

1951

THIS IS
W85



Mont 21

8854



THE EXPERIMENTAL DETERMINATION OF THE BENDING AND
TORSIONAL STIFFNESS OF A BEAM WITH ROTATIONALLY
CONSTANT MOMENT OF INERTIA WITH VARYING AMOUNTS OF
PERMANENT TWIST.

by

LIEUTENANT (Junior Grade) JOHN WOOLSTON, U. S. Navy
B.S., MASS. INST. OF TECH., 1944

LIEUTENANT (Junior Grade) LEON H. LEUTZ, U. S. Navy
B.S., UNIV. OF MICHIGAN, 1945

SUBMITTED IN PARTIAL FULFILLMENT OF THE
REQUIREMENTS FOR THE DEGREE OF
NAVAL ENGINEER.

from the

MASSACHUSETTS INSTITUTE OF TECHNOLOGY

1951

ABSTRACT

Title of Thesis: "The Experimental Determination of the Bending and Torsional Stiffness of a Beam with Rotationally Constant Moment of Inertia with Varying Amounts of Permanent Twist."

Authors: Lieutenant (J.G.) John Woolston, U. S. Navy.
Lieutenant (J.G.) Leon H. Leutz, U. S. Navy.

Submitted for the degree of Naval Engineer in the Department of Naval Architecture and Marine Engineering on May 18, 1951.

The object of this thesis was to investigate the variation of bending and torsional stiffness of a beam with permanent twist. The mild steel beam was cruciform in cross section with webs 0.102" thick and a total depth of 1.503" with .200" fillet radii at the center. The beam length was 50 inches. The effects noted on this beam must modify calculations for other twisted beams such as propeller blades, pump rotors, turbine blades, etc.

The torsional stiffness was calculated from the elastic angle of twist in the beam length under a constant torsional moment. The bending stiffness was calculated from bending deflections measured with the beam acted up on by constant bending moments. Bending stresses were in the elastic range.

The torsional stiffness increased with permanent twist approximately as the square of the helical angle of the outer beam fibers. The stiffness was doubled at a helical angle of 0.27 radians. This checked rather closely with the results of previous theoretical work. The overall results of the torsion tests conform to theory for cross sections approximating simple finned members.

This is known as "the experimental determination of the bending and
torsional stiffness of a beam with boundary conditions
of fixed end, free end, and fixed end."

Equation (1.1) is the bending
Equation (1.2) is the torsion

Equation (1.3) is the degree of freedom of the beam
Equation (1.4) is the degree of freedom of the beam

The object of this paper was to investigate the relation of bending

and torsional stiffness of a beam with boundary conditions. The main result

was that the bending stiffness of a beam with fixed end and a free

end of 1.50" with 1.00" fixed end at the center. The main result

was that the bending stiffness of a beam with fixed end and a free

end of 1.50" with 1.00" fixed end at the center. The main result

was that the bending stiffness of a beam with fixed end and a free

end of 1.50" with 1.00" fixed end at the center. The main result

was that the bending stiffness of a beam with fixed end and a free

end of 1.50" with 1.00" fixed end at the center. The main result

was that the bending stiffness of a beam with fixed end and a free

end of 1.50" with 1.00" fixed end at the center. The main result

was that the bending stiffness of a beam with fixed end and a free

end of 1.50" with 1.00" fixed end at the center. The main result

was that the bending stiffness of a beam with fixed end and a free

end of 1.50" with 1.00" fixed end at the center. The main result

was that the bending stiffness of a beam with fixed end and a free

end of 1.50" with 1.00" fixed end at the center. The main result

In the bending tests the ratio of deflection to the theoretical deflection, based on simple beam theory, increased approximately as the cube of the helical angle to a value of helical angle of about 0.15 radians. This indicates that the beam becomes less stiff as the helical angle increases. At higher angles of twist the curve droops, reaching a maximum deflection ratio of 1.32 at a helical angle of 0.23 radians. The last experimental point showed a deflection ratio of 1.20 at a helical angle of 0.314.

The results of the bending tests show quantitatively the effect of twist on bending stiffness of a member of a particular section. Because this effect is large and its cause unknown it is obvious that much more experimental and theoretical work must be done to establish theories for the many applications of twisted beams in practice.

in the meeting were the ratio of collection to the distribution

collection, based on weight, based on quantity, based on value, etc.

The ratio of the collection to the value of the collection was 0.15

value. This ratio was 0.15 for the collection of value and the collection

ratio was 0.15 for the collection of value and the collection ratio

ratio was 0.15 for the collection of value and the collection ratio

The last ratio (value) ratio was 0.15 for the collection ratio of 0.15

ratio of 0.15.

The results of the meeting were as follows:

of the ratio of the collection to the value of the collection was 0.15

ratio was 0.15 for the collection of value and the collection ratio

ratio was 0.15 for the collection of value and the collection ratio

ratio was 0.15 for the collection of value and the collection ratio

Cambridge, Massachusetts
18 May, 1951

Professor J. S. Newell
Secretary of the Faculty
Massachusetts Institute of Technology
Cambridge, Massachusetts

Dear Sir:

In accordance with the requirements for the Degree of Naval Engineer, we submit herewith a thesis entitled "The Experimental Determination of the Bending and Torsional Stiffness of a Beam with Rotationally Constant Moment of Inertia with varying amounts of Permanent Twist."

Respectfully,

ACKNOWLEDGEMENT

The authors are deeply indebted to Professor J. P. DenHartog of the Massachusetts Institute of Technology whose inspiration and guidance made this thesis possible.

ALPHABETICALLY

The system is being tested in various parts of the country and the results are being reported to the Bureau. The system is being tested in various parts of the country and the results are being reported to the Bureau. The system is being tested in various parts of the country and the results are being reported to the Bureau.

Very truly yours,
[Signature]
[Name]
[Title]

TABLE OF CONTENTS

	<u>Page</u>
ABSTRACT (Summary)	1
NOMENCLATURE	1
INTRODUCTION	2
PROCEDURE	6
RESULTS	15
DISCUSSION OF RESULTS	21
CONCLUSIONS AND RECOMMENDATIONS	24
<u>APPENDIX</u>	
A. Application of the Membrane Analogy	26
B. Data	29
C. Sample Calculations	32
D. Bibliography	33

TABLE OF CONTENTS

Page

1 (Introduction)
2 (Preliminary)
3 (Theoretical)
4 (Experimental)
10 (Results)
11 (Discussion of Results)
12 (Conclusions and Recommendations)
 (Appendix)
21	A. Application of the Theoretical Analysis
22	B. Data
23	C. Theoretical Calculations
24	D. Bibliography

LIST OF ILLUSTRATIONS

Page

FIGURE I	The Arrangement of the beam during Bending Tests	4
FIGURE II	Close-up of the Beam at $\beta_0 = 0.314$	5
FIGURE III	Beam Arrangement in Bending Tests	11
FIGURE IV	Design Dimensions of Beam and Fittings	12
FIGURE V	Micrometer Readings of Beam Dimensions	13
FIGURE VI	Strain Gage Data and Location	14
FIGURE VII	Torsional Stiffness vs. Helical Angle	16
FIGURE VIII	Table of Torsion Data and Results	17
FIGURE IX	Bending Stiffness vs. Helical Angle	18
FIGURE X	Table of Displacements of Point 3 and Support Point from Point 2, Center of Beam	19
FIGURE XI	Bending Deflection Notations	20
FIGURE XII	Portion of Beam Cross Section Showing Stations used in Calculating Membrane Volume used with Membrane Analogy	28
FIGURE XIII	Deflection Readings in Inches at Various Stations, Values of β_0 , and Values of Load	30
FIGURE XIV	Strain Gage Readings in Micro Inches per Inch for Various Values of β_0 and for Various Loads	31

LIST OF ILLUSTRATIONS

Page

FIGURE I	The relationship of the above factors	1
FIGURE II	Diagram of the beam of $P_0 = 0.514$	2
FIGURE III	Beam arrangement in tunnel tests	3
FIGURE IV	Design dimensions of beam and wings	12
FIGURE V	Interference fringes of beam diffraction	13
FIGURE VI	Beam edge light and position	14
FIGURE VII	Location of beam at initial angle	15
FIGURE VIII	Table of beam data and results	17
FIGURE IX	Beam position vs. initial angle	18
FIGURE X	Table of diffraction of beam at initial angle	19
FIGURE XI	Beam position vs. initial angle	20
FIGURE XII	Position of beam at initial angle	21
FIGURE XIII	Diagram of beam at initial angle	22
FIGURE XIV	Table of beam data and results	23
FIGURE XV	Beam position vs. initial angle	24
FIGURE XVI	Table of beam data and results	25
FIGURE XVII	Beam position vs. initial angle	26
FIGURE XVIII	Table of beam data and results	27
FIGURE XIX	Beam position vs. initial angle	28
FIGURE XX	Table of beam data and results	29
FIGURE XXI	Beam position vs. initial angle	30
FIGURE XXII	Table of beam data and results	31
FIGURE XXIII	Beam position vs. initial angle	32
FIGURE XXIV	Table of beam data and results	33
FIGURE XXV	Beam position vs. initial angle	34
FIGURE XXVI	Table of beam data and results	35
FIGURE XXVII	Beam position vs. initial angle	36
FIGURE XXVIII	Table of beam data and results	37
FIGURE XXIX	Beam position vs. initial angle	38
FIGURE XXX	Table of beam data and results	39
FIGURE XXXI	Beam position vs. initial angle	40
FIGURE XXXII	Table of beam data and results	41
FIGURE XXXIII	Beam position vs. initial angle	42
FIGURE XXXIV	Table of beam data and results	43
FIGURE XXXV	Beam position vs. initial angle	44
FIGURE XXXVI	Table of beam data and results	45
FIGURE XXXVII	Beam position vs. initial angle	46
FIGURE XXXVIII	Table of beam data and results	47
FIGURE XXXIX	Beam position vs. initial angle	48
FIGURE XXXX	Table of beam data and results	49
FIGURE XXXXI	Beam position vs. initial angle	50
FIGURE XXXXII	Table of beam data and results	51
FIGURE XXXXIII	Beam position vs. initial angle	52
FIGURE XXXXIV	Table of beam data and results	53
FIGURE XXXXV	Beam position vs. initial angle	54
FIGURE XXXXVI	Table of beam data and results	55
FIGURE XXXXVII	Beam position vs. initial angle	56
FIGURE XXXXVIII	Table of beam data and results	57
FIGURE XXXXIX	Beam position vs. initial angle	58
FIGURE XXXXX	Table of beam data and results	59
FIGURE XXXXXI	Beam position vs. initial angle	60
FIGURE XXXXXII	Table of beam data and results	61
FIGURE XXXXXIII	Beam position vs. initial angle	62
FIGURE XXXXXIV	Table of beam data and results	63
FIGURE XXXXXV	Beam position vs. initial angle	64
FIGURE XXXXXVI	Table of beam data and results	65
FIGURE XXXXXVII	Beam position vs. initial angle	66
FIGURE XXXXXVIII	Table of beam data and results	67
FIGURE XXXXXIX	Beam position vs. initial angle	68
FIGURE XXXXXX	Table of beam data and results	69
FIGURE XXXXXXI	Beam position vs. initial angle	70
FIGURE XXXXXXII	Table of beam data and results	71
FIGURE XXXXXXIII	Beam position vs. initial angle	72
FIGURE XXXXXXIV	Table of beam data and results	73
FIGURE XXXXXXV	Beam position vs. initial angle	74
FIGURE XXXXXXVI	Table of beam data and results	75
FIGURE XXXXXXVII	Beam position vs. initial angle	76
FIGURE XXXXXXVIII	Table of beam data and results	77
FIGURE XXXXXXIX	Beam position vs. initial angle	78
FIGURE XXXXXX	Table of beam data and results	79
FIGURE XXXXXXI	Beam position vs. initial angle	80
FIGURE XXXXXXII	Table of beam data and results	81
FIGURE XXXXXXIII	Beam position vs. initial angle	82
FIGURE XXXXXXIV	Table of beam data and results	83
FIGURE XXXXXXV	Beam position vs. initial angle	84
FIGURE XXXXXXVI	Table of beam data and results	85
FIGURE XXXXXXVII	Beam position vs. initial angle	86
FIGURE XXXXXXVIII	Table of beam data and results	87
FIGURE XXXXXXIX	Beam position vs. initial angle	88
FIGURE XXXXXXX	Table of beam data and results	89
FIGURE XXXXXXXI	Beam position vs. initial angle	90
FIGURE XXXXXXXII	Table of beam data and results	91
FIGURE XXXXXXXIII	Beam position vs. initial angle	92
FIGURE XXXXXXXIV	Table of beam data and results	93
FIGURE XXXXXXXV	Beam position vs. initial angle	94
FIGURE XXXXXXXVI	Table of beam data and results	95
FIGURE XXXXXXXVII	Beam position vs. initial angle	96
FIGURE XXXXXXXVIII	Table of beam data and results	97
FIGURE XXXXXXXIX	Beam position vs. initial angle	98
FIGURE XXXXXXX	Table of beam data and results	99
FIGURE XXXXXXXI	Beam position vs. initial angle	100

NOMENCLATURE

- L = Length of beam from load to load or 50".
- L' = Length of beam used in measurement of torsional stiffness in inches.
- α = Angle of permanent twist in the beam in degrees.
- ϕ = Angle of elastic twist of the beam under the action of torsional moment, T , where the moment was applied to the beam over a length L' ; ϕ in degrees.
- β_0 = Helical angle of outer fiber of the beam = $\frac{\alpha \times r_0}{57.3 \times L}$ radians.
- r_0 = Radius of the outer fiber of the beam in inches or 0.751".
- J = Torsional stiffness of the beam, T/θ
- J/J_s = Ratio of the torsional stiffness of the twisted beam to that of the straight beam.
- T = Torsional moment, inch pounds.
- θ = Angle of elastic twist per unit length as a result of the torsional moment; radians per unit length.
- Δ = Displacement of a point on the beam when loaded, measured from the unloaded position.
- δ = Displacement of a point on the loaded beam from the tangent at the center of the beam, corrected for lack of straightness in the unloaded beam.
- δ_0 = Theoretical displacement from horizontal tangent at center of beam, based on simple beam theory.
- δ/δ_0 = Ratio of displacement of beam to theoretical displacement.
 $\delta/\delta_0 = (EI)_0 / EI =$ ratio of original stiffness to stiffness at a given angle of permanent twist.

- [illegible]

INTRODUCTION

Conventional beam theory states that if the EI product of a beam is constant, that is the stress-strain relationship is linear and the moment of inertia does not change, the beam will maintain the same bending stiffness, EI . Under these conditions the beam will always deflect the same amount under identical loadings.

The question then arises as to what happens to the bending stiffness when the beam has a longitudinal twist. If the modulus of elasticity is constant and the section has a rotationally constant moment of inertia, that is the I is the same about all axis through the center of gravity of the beam section, will the beam theory break down for a twisted beam? In the case of helical pump impellers and also in airplane propellers with their inherent pitch this question of twisted beams arises. The pump impeller designer will want to know the impeller stiffness for strength and for vibration characteristics. The propeller designer will pose the same questions concerning his design.

As far as is known no experimental or theoretical work has been done on the above question of bending stiffness. However, it is the belief of some engineers that the bending stiffness is not the same for a twisted beam as for a straight beam with the same EI . In one instance the designers of airplane propellers find it difficult to calculate the exact natural frequency of vibration of the blades and their results may be 15% in error from the actual value. This error may be due to using an incorrect value of the bending stiffness of the blade because

Commercial banks have been told that it is a matter of a week

is evident that the situation is becoming more and more

moment of time and change for them will maintain the same

leading position, but they have realized the fact that they will

the same amount of business.

The position that they are in now is very different from the position

when they were in a position of strength. It is now a matter of

strength and the position has a completely different character

that is the fact that they are now in a position of

the same position will be in a position of a weak position

in the case of the bank which is in a position of

with them because they are in a position of a weak position

and they are in a position of a weak position

stronger and in a position of a weak position. The position

will not be the same position concerning the bank.

As far as the bank is concerned in the position of a weak

position and in a position of a weak position. However, it is

the fact that the bank is in a position of a weak position

for it is in a position of a weak position with the bank. It is

because the position of the bank is in a position of a weak

the bank is in a position of a weak position and it is in a

may be it is in a position of a weak position. The bank is in a

and in a position of a weak position of the bank because

they do not account for the twist.

The experimental determination of the variation of bending stiffness vs. angle of permanent twist is then begun without knowing the nature of the possible results or if there are any variations whatever. It is known, however, that in applying the angle of permanent twist to the beam that the outer fibers will be yielded in tension and the inner fibers will be yielded in compression. However, during the bending tests, since the beam is free to change its length longitudinally, the state of longitudinal stress will be well below the yield stress after the twisting moment is removed even though the beam has been yielded. The stress pattern of the beam will be quite complicated because of the bending stresses being superimposed upon the stresses that have been set up during the application of the permanent twist. It is felt that the latter stresses will have little effect upon the stiffness of the beam as long as the total stress is kept below the proportional limit. If there is a change in bending stiffness with changing angles of permanent twist it is most likely due to the interaction of the stresses caused by the geometry of the beam.

The other major topic to be examined here is the variation of the torsional stiffness of a beam as the angle of permanent twist is varied. This subject has been theoretically and experimentally studied and a bases for a comparison of results is at hand. Let it suffice to say that the torsional stiffness will increase with the angle of permanent twist and that for a rectangular beam this increase is primarily a function of the square of the height to thickness ratio of the beam cross section.

They are not known for the truth.

The psychological consequences of the violation of family and-

ness are, again, of enormous value, it is not known without knowing the history

of the family system as it exists in the present moment. It is

known, however, that in the light of the present facts in the

fact that the present facts will be present in the future and the future

will be present in the present. However, noting the present facts, some

the point is to change the family (psychologically), the state of the family

system will be well before the fact where the state of the family system is

removed even though the system has been changed. The present picture of

the system will be a more complete picture of the family system being

expected from the system that has been set up by the system

and of the system itself. It is not that the future system will have

little effect upon the system in the future as long as the present system is

not being the psychological fact. It is not a change in the present will-

ness with the psychological system of the present but it is not likely due to

the operation of the system created by the system of the present.

The more major point in the present is the violation of

the system itself as a point in the system of the present but it is not

This subject was not theoretically and experimentally studied and a

basis for a comparison of results is at hand. Let it suffice to say that

the present system will be a more complete picture of the family system

and that for a psychological basis that system is primarily a function of the

system of the family in the present (the present system).

FIGURE I

THE ARRANGEMENT OF THE BEAM DURING BENDING TESTS

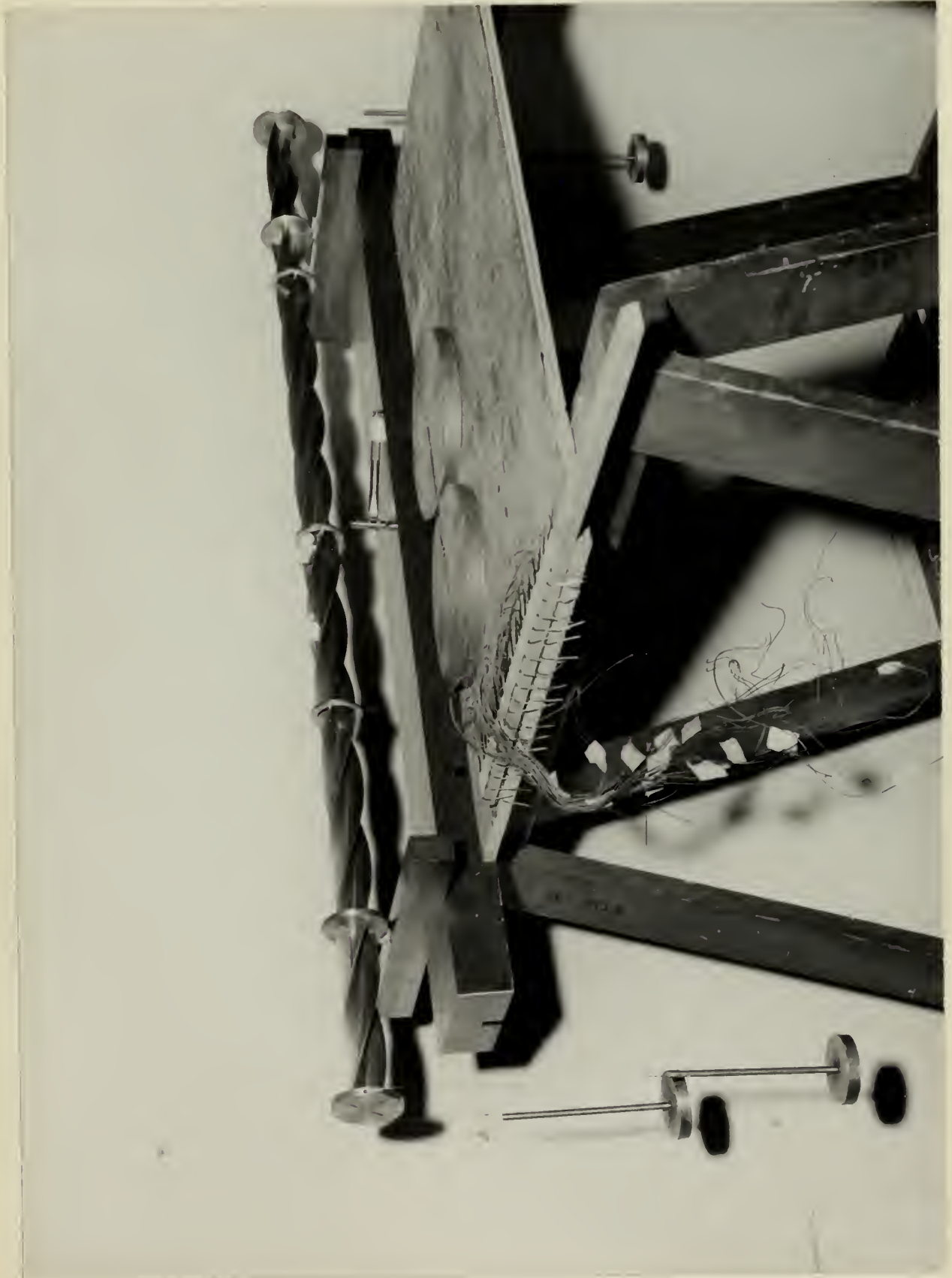


FIGURE II
CLOSE-UP OF THE BEAM AT $\beta_0 = .314$



PROCEDURE

The beam shown in Figure IV was designed with a rotationally constant moment of inertia in order that the conditions of the thesis could be met. The beam dimensions were chosen on the basis of predictable results to be obtained from the laboratory technique employed. The bending stiffness of the beam was to be obtained from the deflection of the beam loaded as shown in Figure III. This loading produces a constant bending moment on the beam between the supports. These deflections, to be measured with an inside micrometer (see Figure I), were to have an approximate maximum value of .100" at the center of the beam while keeping the stress in the beam well below the yield stress of the material, mild steel, or about 15,000 psi. The .100" maximum deflection figure was chosen since it was felt that an error of .001" would have to be accepted in the deflection measurements. This then would limit the error to 1% at the maximum deflection point. Furthermore, the loads to be used on the beam would have to be of a size that could be readily applied in the laboratory.

In order to obtain the variation of bending stiffness with the angle of permanent twist the beam was to be given additional twist prior to each run. Since there were no mechanical means of applying this twist available it would have to be applied manually. This condition further dictated the beam dimensions but it was found by using the membrane analogy that this condition of manual twisting of the beam did not necessitate a change in the beam dimensions derived from the above

PROCEDURE

The beam shown in Figure IV was designed with a rotationally constant moment of inertia in order that the conditions of the flexure could be met. The beam dimensions were chosen on the basis of predictable results to be obtained from the laboratory technique employed. The bending stress area of the beam was to be obtained from the deflection of the beam loaded as shown in Figure III. This loading produces a constant bending moment on the beam between the supports. These deflections, to be measured with an inside micrometer (see Figure II), were to have an approximate maximum value of .100" at the center of the beam while keeping the stress in the beam well below the yield stress of the material, mild steel, or about 15,000 psi. The .100" maximum deflection figure was chosen since it was felt that an error of .001" would have to be accepted in the deflection measurements. This then would limit the error to 1% of the maximum deflection point. Furthermore, the loads to be used on the beam would have to be of a size that could be readily applied in the laboratory.

In order to obtain the variation of bending stiffness with the angle of permanent twist the beam was to be given additional twist prior to each run. Since there were no mechanical means of applying this twist available it would have to be applied manually. This condition further dictated the beam dimensions but it was found by using the membrane analogy that this condition of manual twisting of the beam did not necessitate a change in the beam dimensions derived from the above

bending criteria. The final beam design is shown in Figure IV.

The beam and its fittings were manufactured at the Boston Naval Shipyard. It was planed from solid stock, heat treated and planed to its final dimensions. Because of the length of the beam and the play in the planer head it was found that the design tolerances could not be met. The beam micrometer readings are shown in Figure V. From these readings a mean value of flange thickness was taken as .1020" and mean beam depth of 1.5030". The moment of inertia of the section was calculated from these mean values and found to be .02925 in.⁴. The support rings, load rings and deflection rings were hand filed and fitted to the beam snugly with a hand fit. The bed plate was surface ground to a smooth finish.

The procedure used in the deflection tests is shown in Figure I where the supports are set up on parallels so that an inside micrometer might be used to measure the deflections. In the no load condition only the load rings (pulleys) were in place and deflections were read at each deflection ring between the supports. To apply the loads the weight supports (shown) were hung over the load rings and equal load weights, calibrated to .01#, were placed on the supports. Each separate weight (note two weights on table in Figure I) was $11.03 \pm .01\#$ and the weight supports weighed 1.39# at each end of the beam. The weight supports were designed so that no torsional moment would be applied to the beam when the load was applied. For each load condition 4 weights were placed on the beam, two at each end. The deflection rings were placed

ending criteria. The final beam design is shown in Figure IV.

The beam and its findings were summarized as the design beam.

It was found from solid stress, beam treated and placed in its final dimension. Because of the length of the beam and the play in the beam head it was found that the design tolerances could not be met.

The beam instrument readings are shown in Figure V. From these

readings a mean value of beam thickness was taken as .1020" and

mean beam depth of .1030". The moment of inertia of the section was

calculated from these mean values and found to be .0215 in⁴. The

support rings, load rings and deflection rings were hand filed and fitted

to the beam snugly with a hand fit. The test plate was surface ground

to a smooth finish.

The procedure used in the deflection tests is shown in Figure I

where the supports are set up on parallels and an inside micrometer

might be used to measure the deflection. In the no load condition only

the load rings (collars) were in place and deflections were read at each

deflection ring between the supports. To apply the loads the weights

supports (shown) were hung over the load rings and equal load weights

calibrated to .014, were placed on the supports. Each support weight

(and two weights on table in Figure I) was 1.03 ± .014 and the weight

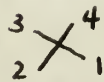
supports weighed .124 at each end of the beam. The weight supports

were designed so that no torsional moment would be applied to the beam

when the load was applied. For each load condition 4 weights were

placed on the beam, two at each end. The deflection rings were placed

to give a spread of readings. Deflection ring 3 was placed 3" from the support, or two beam diameters distance so that the effect of the support would not be felt. This is in accordance with Saint Venant's principle.

The beam stiffness in bending was checked in two rotational positions. The initial position of the beam was with flange 3 vertically up at the mid-span of the beam. No load and loaded beam deflections were taken with the beam in this position. When the beam was unloaded it was rolled through 45° with flanges 3 and 4 thus:  when looking at the beam from the left end in Figure III. At Run 15, when the largest value of β_0 was reached, the beam deflection was read with flange 3 at mid-span rotated through 360° with readings taken at each 45° interval. This beam rotation was accomplished to ascertain if the stiffness varied with the beam position on the supports. It seemed likely that if the beam stiffness varied with the angle of permanent twist that it might also vary with the position of the beam on the supports.

Strain gages, as shown in Figure VI, were placed on the beam to give possible aid in the analysis of results. These gages were all placed to indicate longitudinal strain near the outer fibers of the flanges in order that a longitudinal stress distribution might be had with the beam in a twisted condition. These gages were read only during the bending tests.

The beam was received in the straight condition from the Boston Naval Shipyard. The initial, straight beam deflection tests were made

to give a spread of readings. The beam was tilted 1" from the support by two lead bricks placed at the feet of the support and not at the feet. This is in accordance with the principle of the experiment.

The beam support is shown in the photograph. The initial position of the beam was with the beam 1 vertically up at the mid-point of the beam. The beam and loaded beam deflection were taken with the beam in this position. When the beam was rotated it was rotated through 45° with flanges 1 and 2 down, 3 and 4 up, looking at the beam from the left and in Figure III. At this time the largest value of A was recorded, the beam deflection was read with flange 1 at mid-point rotated through 45° with readings taken at each 45° interval. This beam rotation was accomplished by securing it by the beam with the beam parallel to the support. It seemed likely that if the beam deflection varied with the angle of curvature, it would be the same for all the positions of the beam. It might also vary with the position of the beam on the support.

Beam deflection was shown in Figure VI. The beam was placed on the beam to give possible aid in the analysis of results. These pages were all placed to indicate longitudinal strain near the outer fibers of the flanges in order that a longitudinal stress distribution might be had with the beam in a rotated condition. These pages were read only during the bending tests.

The beam was rotated to the straight condition from the position shown in Figure VI. The initial straight beam deflection tests were made

and checked against the calculated values found by using standard beam theory. In order to determine the modulus of elasticity of the material a tensile test specimen was made by the shipyard and given the same heat treatment as the beam. A stress-strain curve was made from a tensile test and the modulus of elasticity was found to be 29.7×10^6 psi. The material had a proportional limit of 24,500 psi and an ultimate stress of 56,900 psi.

The torsional stiffness was found with the beam in the straight condition. This was done by holding the beam fixed at one end and applying a twisting moment at the other end. A twisting moment of 124.3 in. lbs. was used and the shear stresses set up in the beam were well within the elastic region of the beam material. The beam was held at one end by fastening a die stock to the load ring and holding the arms of the stock firmly to a stationary support. On the other end the load ring had been drilled and tapped (note holes in support ring at far end in Figure I) symmetrically so that an arm could be fitted to it. This arm was grooved 10" from the center of the beam thus giving the arm of the moment. From this groove the load supports were hung along with one lead weight, or a total of 12.43#. With this load applied the arm was made to be horizontal by setting the position of the die stock at the other end. Therefore, the full moment acted on the beam. The load was then removed and the angle through which the beam untwisted with the other end fixed was measured by using a protractor. This made possible the calculation of the torsional stiffness. This test was

and another against the vertical axis (load by using standard beam
theory). In order to determine the position of the vertical axis
relative to the beam, the beam was loaded by the support and the beam
positioned at the beam. A support beam was used to support a beam
and the position of the beam was found to be 10.7 x 10⁻³ m. The
vertical axis was a vertical line of 10.7 x 10⁻³ m and the vertical axis
of 10.7 x 10⁻³ m.

The vertical axis was found with the beam in the vertical
condition. This was done by holding the beam fixed at the end and
applying a twisting moment at the other end. A twisting moment of
10.7 x 10⁻³ m was used and the beam was not at the beam was
well within the elastic region of the beam material. The beam was
fixed at the end by holding it in the beam and holding the
beam of the beam fixed in a slightly support. On the other end the
beam was fixed and the beam was fixed (the beam is fixed at the
end of the beam) so that the beam could be fixed to it. This
axis was proposed to be the center of the beam that gives the
of the beam. From this point the load supports were measured
with one end fixed at a point in the beam with the beam applied the
axis was made in the beam by twisting the beam of the beam
at the other end. Therefore, the beam was fixed at the beam. The
beam was fixed and the beam was fixed (the beam is fixed at the
with the beam and fixed with the beam by using a support. This
axis was made in the beam by twisting the beam of the beam

also run with the beam on the bed plate.

The next phase was to apply a permanent twist to the beam. This was done by fastening the die stock to the load ring on one end of the beam and using the arm on the other end. The beam was placed freely on the bed plate and manually given a permanent twist. The beam was maintained straight by the bed plate in vertical plane but could possibly bend somewhat in the horizontal plane. But by carefully applying this torsional moment the bending of the beam could be minimized and it was found to be very small. Figure VIII shows the amounts of permanent twist put into the beam with each run.

With permanent twist in the beam the deflection and torsional tests were again made in the same manner as described above. The amount of permanent twist applied to the beam was to be small at the offset so that the initial trend of the stiffness curves could be accurately determined. After this trend had been found the angle of permanent twist between runs was increased as shown in Figure VIII. Permanent twist was applied to the beam up to the point where it became too stiff to twist manually. It was also necessary to check to see if the beam flanges warped from the twisting since if they did the moment of inertia of the section would be reduced. This was done by checking to see if the flanges were still at right angles and also by the tightness of the deflection rings on the beam.

also run with the water on the bed plate.

The next phase was to supply a permanent water to the bed.

was done by fastening the bed to the bed plate and by the beam

and using the water on the bed plate. The beam was placed freely on the

bed plate and manually given a permanent water. The beam was indicated

weight by the bed plate in which the beam was placed freely on the

what is the horizontal plate. But by carefully applying this horizontal

moment the beam of the beam would be horizontal and it was found to

be very small. Figure 11 shows the moment of horizontal water

into the beam with each run.

The permanent water in the beam the deflection and horizontal

water were again made in the same manner as described above. The

moment of horizontal water applied to the beam was in the water at the end

was so that the beam of the deflection curve could be accurately

determined. After this it was found that the water of horizontal

water between the beam was increased as shown in Figure 11. The

water was applied to the beam of the beam where it is shown in the

to water manually. It was also necessary to check to see if the beam

finger-wiper from the twisting plate to the beam of the beam of the

of the beam would be removed. This was done by checking to see if

the finger were still at right angles and also by the rightness of the

deflection curve on the beam.

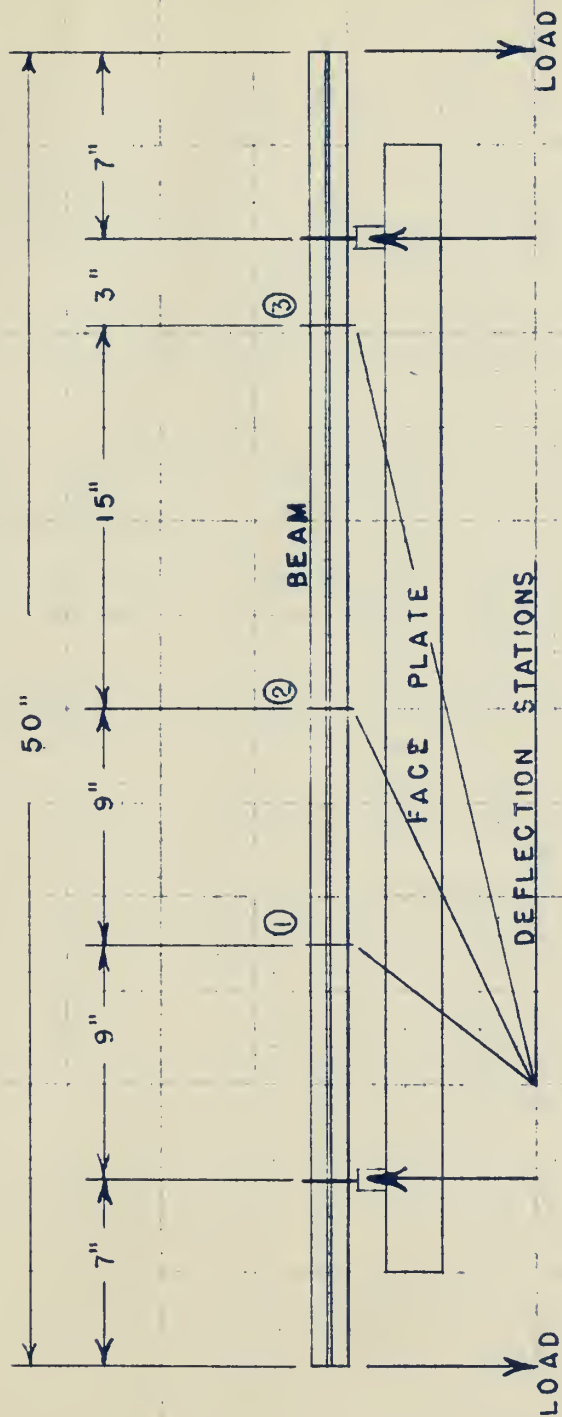


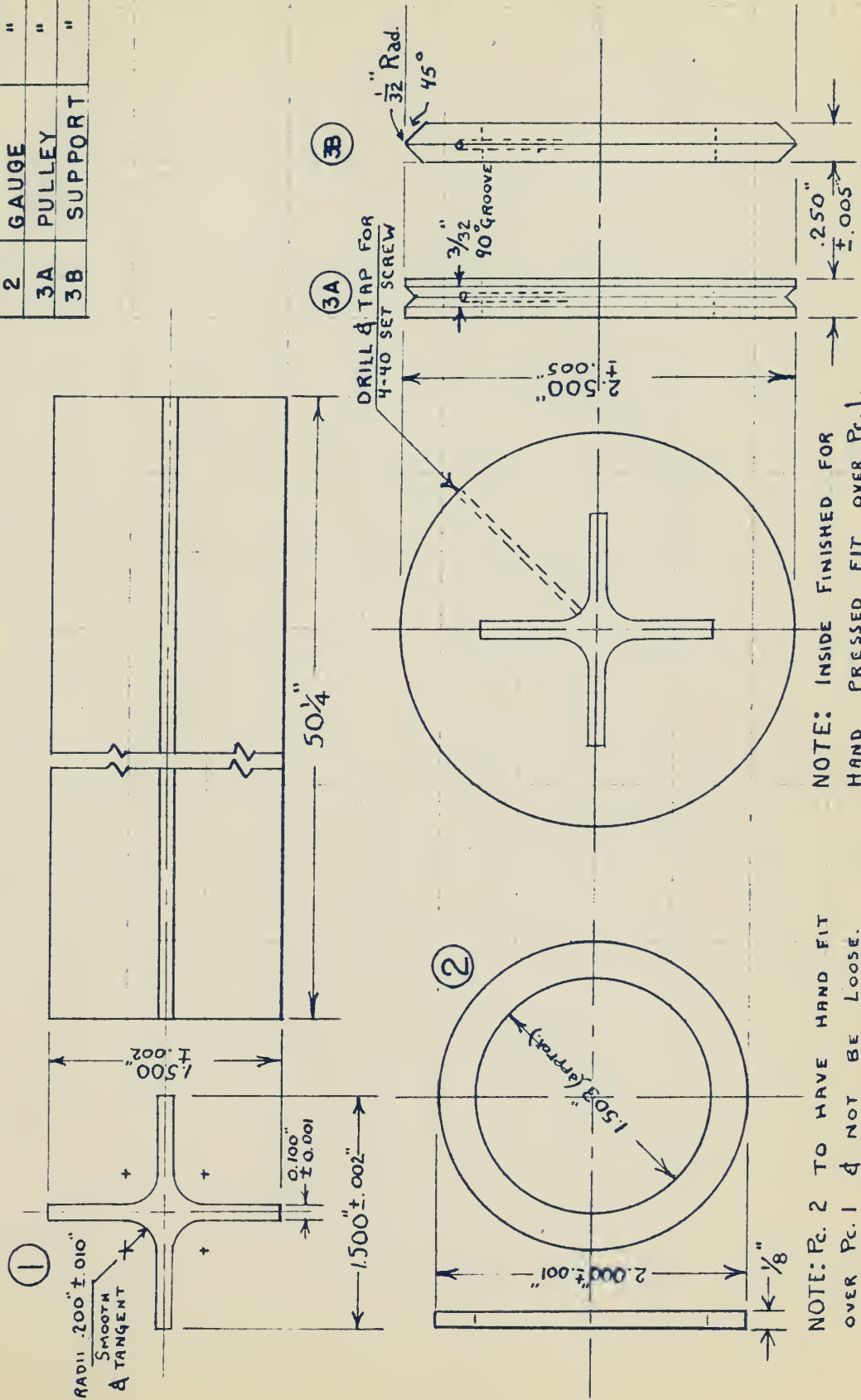
FIGURE III
BEAM ARRANGEMENT
IN BENDING TESTS

gaw
dhd
4-18-51

FIGURE IV

DESIGN DIMENSIONS OF
BEAM AND FITTINGS.

BILL OF MATERIAL		
P.C.	ITEM	MATERIAL
1	BEAM	COLD ROLLED MILD STEEL
2	GAUGE	"
3A	PULLEY	"
3B	SUPPORT	"



NOTE: P.C. 2 TO HAVE HAND FIT
OVER P.C. 1 & NOT BE LOOSE.

NOTE: INSIDE FINISHED FOR
HAND PRESSED FIT OVER P.C.1.

fw
JHJ
4-18-51

FIGURE V

MICROMETER READINGS OF BEAM DIMENSIONS.

STATION	FLANGE THICKNESS				BEAM DEPTH	
	Fl.#1	Fl.#2	Fl.#3	Fl.#4	Fls.1-3	Fls.2-4
0	.1023	.1017	.1023	.1030	1.5002	1.5033
1	.1003	.1008	.1015	.1002	1.5017	1.5035
2	.1006	.1010	.1016	.1010	1.5021	1.5041
3	.1014	.1018	.1028	.1025	1.5030	1.5047
4	.1015	.1024	.1033	.1021	1.5028	1.5040
5	.1018	.1012	.1033	.1004	1.5037	1.5037
6	.1023	.1016	.1030	.1013	1.5040	1.5038
7	.1028	.1019	.1040	.1028	1.5040	1.5037
8	.1020	.1016	.1038	.1025	1.5036	1.5032
9	.1010	.1002	.1015	.1006	1.5036	1.5028
10	.1011	.1003	.1015	.1016	1.5030	1.5035

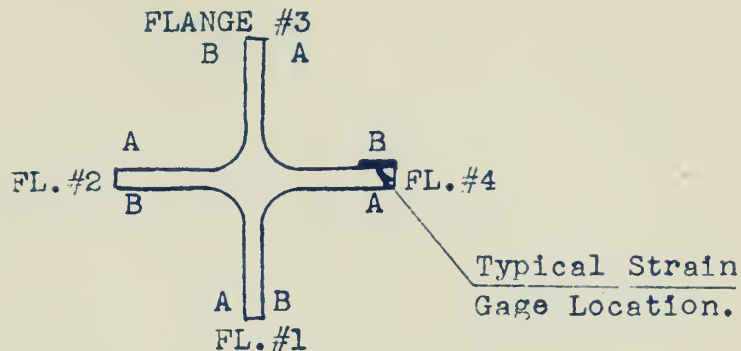
Stations are spaced each 5 inches along length of the beam. Station 0 is at left end of the beam as seen in Figure III.

All measurements are in inches.

Flange thicknesses were measured at the outer edges of the flange.

FIGURE VI

STRAIN GAGE DATA & LOCATION



BEAM CROSS SECTION LOOKING
AT BEAM IN FIGURE III FROM
THE LEFT END

STRAIN GAGE LOCATIONS

The strain gages are designated as to location by the flange number, the flange face letter (A or B) and by their distance in inches from the left end of the beam as shown in Fig. III. Then gage 3A 16 would be on flange 3, on the A face and 16 inches from the left end. All gages were oriented to give longitudinal strain and the center of the gage resistance wires were 0.1" in from the outer edge of the flange.

STRAIN GAGE DATA

Type: A-7
Res. in Ohms: 120
Gage Factor: 1.96
Lot Number: 501
Manufacturer: Baldwin Loco. Works.

fdw
JH2
4-19-51

RESULTS

The results of the torsion tests are shown in figures VII and VIII.

It will be seen that the torsional stiffness increases with increased helical angle in approximately a parabolic manner and that the stiffness ratio J/J_s reaches 2.00 at a β_0 of .27.

The results of the bending tests are shown in figures IX and X.

It will be seen that the displacement ratio δ/δ_0 , which is the reciprocal of the stiffness ratio $(EI)_0/(EI)$, increases with helical angle exponentially to a β_0 of about .15. The exponent in this case is evidently slightly less than 3. Above $\beta_0 = .15$ the rate of increased δ/δ_0 decreases until a maximum value of $\delta/\delta_0 = 1.32$ at $\beta_0 = .23$ is reached. The trend of the results continues with this drooping characteristic to the last experimental point of $\delta/\delta_0 = 1.2$ at $\beta_0 = .314$.

RESULTS

The results of the various tests are shown in Figures 11 and 12. It will be seen that the critical stresses increase with increased values of the exponent n and that the critical stress σ_c is reached at $\epsilon = 0.001$ at $n = 1.5$.

The results of the bending tests are shown in Figure 13 and 14. It will be seen that the displacement ratio δ/ϵ_0 which is the reciprocal of the stiffness ratio $(EI)_0/(EI)$ increases with initial angle exponentially to a δ/ϵ_0 of about 1.5. The exponent in this case is considerably higher than 2. Above $\delta/\epsilon_0 = 1.5$ the rate of increase of δ/ϵ_0 decreases until a maximum value of $\delta/\epsilon_0 = 1.5$ is reached. The trend of the results compares well with the theoretical relationship in the last experimental paper of $\delta/\epsilon_0 = 1.5$ at $\delta/\epsilon_0 = 1.5$.

FIGURE VII
TORSIONAL STIFFNESS
VS.
HELICAL ANGLE

EQUATION (1)
EXPERIMENTAL

800
2HZ
4-20-51

J/J_s

β_0

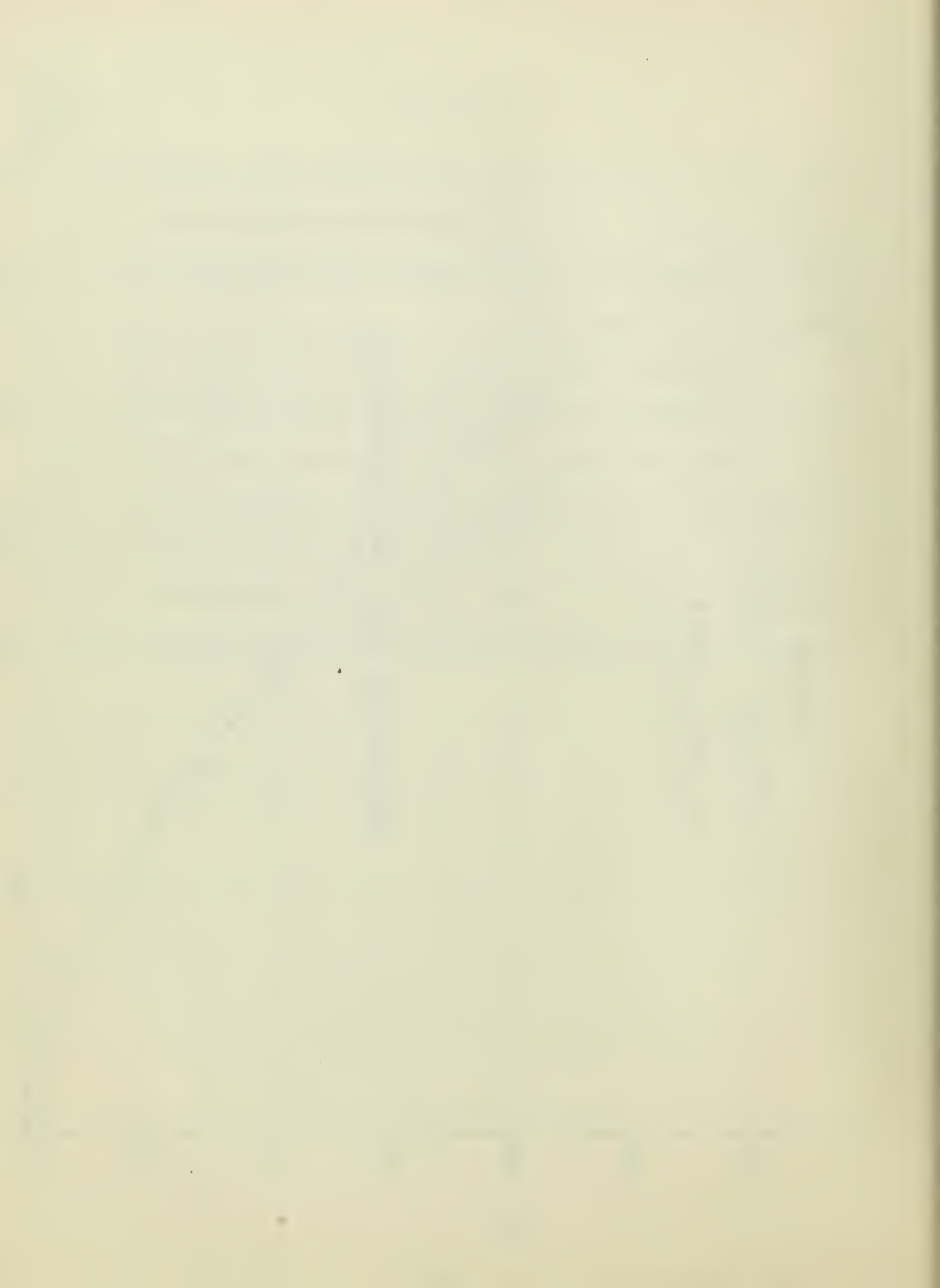


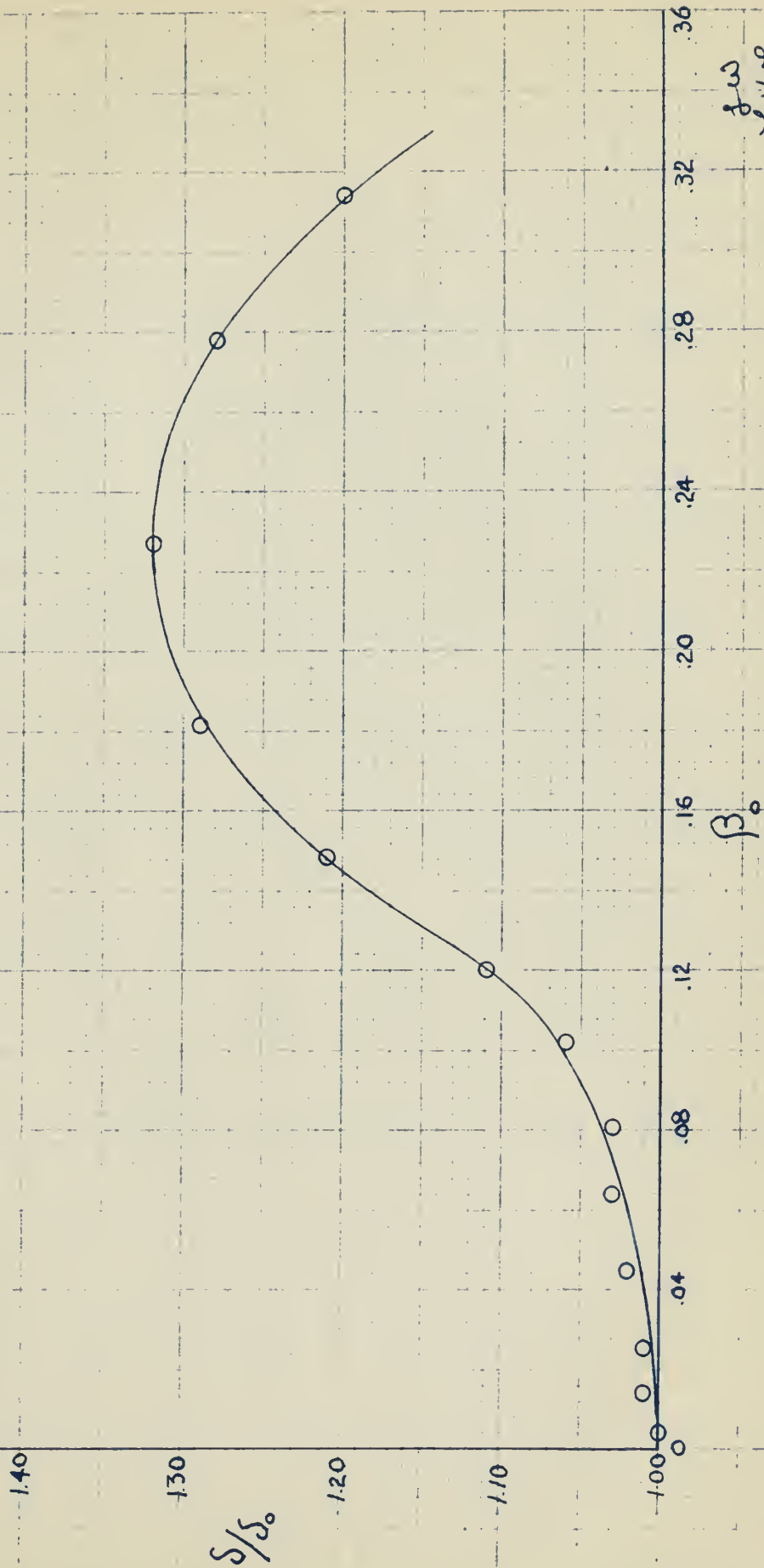
FIGURE VIII
TABLE OF TORSION
DATA & RESULTS

RUN	α°	β_0	ϕ°	L'	Θ	$\frac{J}{J_s} = \frac{.00426}{\Theta}$
1	0	0	11	45.1	.00426	1.000
2	16	.0042	11	45.1	.00426	1.000
3	55	.0144	11	45.1	.00426	1.000
4	98	.0257	11	45.1	.00426	1.000
5	170½	.0477	12	50	.00418	1.018
6	243	.0639	12	50	.00418	1.018
7	307½	.0807	10½	50	.00366	1.162
8	389	.1022	10	50	.00349	1.220
9	458	.1200	9½	50	.00332	1.282
10	567	.1488	8¾	50	.00305	1.395
11	692	.1814	8	50	.00279	1.525
12	866	.227	7	50	.00244	1.744
13	866	.227	7	50	.00244	1.744
14	1063	.278	5½	50	.00192	2.217
15	1199	.314	5½	50	.00192	2.217

JW
JHP
4-19-61

FIGURE IX

BENDING STIFFNESS ($\frac{s}{s_0}$) VS.
HELICAL ANGLE (β_0).



g.w.
J.H.S.
4-19-51

FIGURE X

TABLE OF DISPLACEMENTS OF POINT 3 & SUPPORT
FROM POINT 2; CENTER OF BEAM.

Symbols as shown in Figure X1

X indicates beam rotated 45°.

RUN δ/δ_0	Load	δ_3	δ_5	δ_3/δ_{30}	δ_5/δ_{50}	RUN δ/δ_0	Load	δ_3	δ_5	δ_3/δ_{30}	δ_5/δ_{50}
Theory	Ld.1	.021	.031			RUN 8	Ld.1	.022	.032	1.05	1.03
	Ld.2	.040	.059				Ld.2	.043	.062	1.07	1.05
RUN 1 1.00 X	Ld.1	.021	.030	1.00	.98	1.06 X	Ld.1	.022	.032	1.05	1.03
	Ld.2	.040	.059	1.00	1.00		Ld.2	.043	.062	1.07	1.05
	Ld.1	.021	.031	1.00	1.00	RUN 9 1.11	Ld.1	.023	.034	1.10	1.10
	Ld.2	.040	.059	1.00	1.00		Ld.2	.045	.066	1.12	1.12
RUN 2 1.00 X	Ld.1	.021	.030	1.00	0.97	RUN 10 1.21	Ld.1	.025	.037	1.19	1.19
	Ld.2	.041	.060	1.02	1.02		Ld.2	.050	.072	1.25	1.22
	Ld.1	.021	.030	1.00	0.97	RUN 11 1.29	Ld.1	.027	.040	1.29	1.29
	Ld.2	.040	.060	1.00	1.02		Ld.2	.052	.076	1.30	1.29
RUN 3 1.01 X	Ld.1	.022	.031	1.05	1.00	RUN 12&13 1.32 X	Ld.1	.028	.040	1.33	1.29
	Ld.2	.041	.059	1.02	1.00		Ld.2	.053	.077	1.33	1.31
	Ld.1	.022	.031	1.05	1.00		Ld.1	.028	.041	1.33	1.32
	Ld.2	.040	.059	1.00	1.00		Ld.2	.053	.078	1.33	1.32
RUN 4 1.01 X	Ld.1	.021	.031	1.00	1.00	RUN 14 1.28 X	Ld.1	.027	.040	1.29	1.29
	Ld.2	.041	.059	1.02	1.00		Ld.2	.051	.076	1.27	1.29
	Ld.1	.021	.031	1.00	1.00		Ld.1	.027	.039	1.29	1.26
	Ld.2	.042	.059	1.05	1.00		Ld.2	.051	.075	1.27	1.27
RUN 5 1.02 X	Ld.1	.021	.031	1.00	1.00	RUN 15 1.20 X	Ld.1	.026	.037	1.24	1.19
	Ld.2	.041	.059	1.02	1.00		Ld.2	.048	.072	1.20	1.22
	Ld.1	.022	.031	1.05	1.00		Ld.1	.025	.037	1.19	1.19
	Ld.2	.042	.060	1.05	1.02		Ld.2	.047	.071	1.18	1.20
RUN 6 1.03 X	Ld.1	.022	.032	1.05	1.03	R 16 90°	Ld.1	.025	.037	1.19	1.19
	Ld.2	.043	.061	1.07	1.03	R 17 135°	Ld.1	.025	.037	1.19	1.19
	Ld.1	.021	.031	1.00	1.00	R 18 180°	Ld.1	.026	.037	1.24	1.19
	Ld.2	.041	.060	1.02	1.02	R 19 225°	Ld.1	.025	.037	1.19	1.19
RUN 7 1.03 X	Ld.1	.022	.031	1.05	1.00	R 20 270°	Ld.1	.026	.037	1.24	1.19
	Ld.2	.043	.061	1.07	1.03	R 21 315°	Ld.1	.025	.037	1.19	1.19
	Ld.1	.021	.031	1.02	1.00						
	Ld.2	.041	.060	1.02	1.02						

2W
2H2
4-17-51

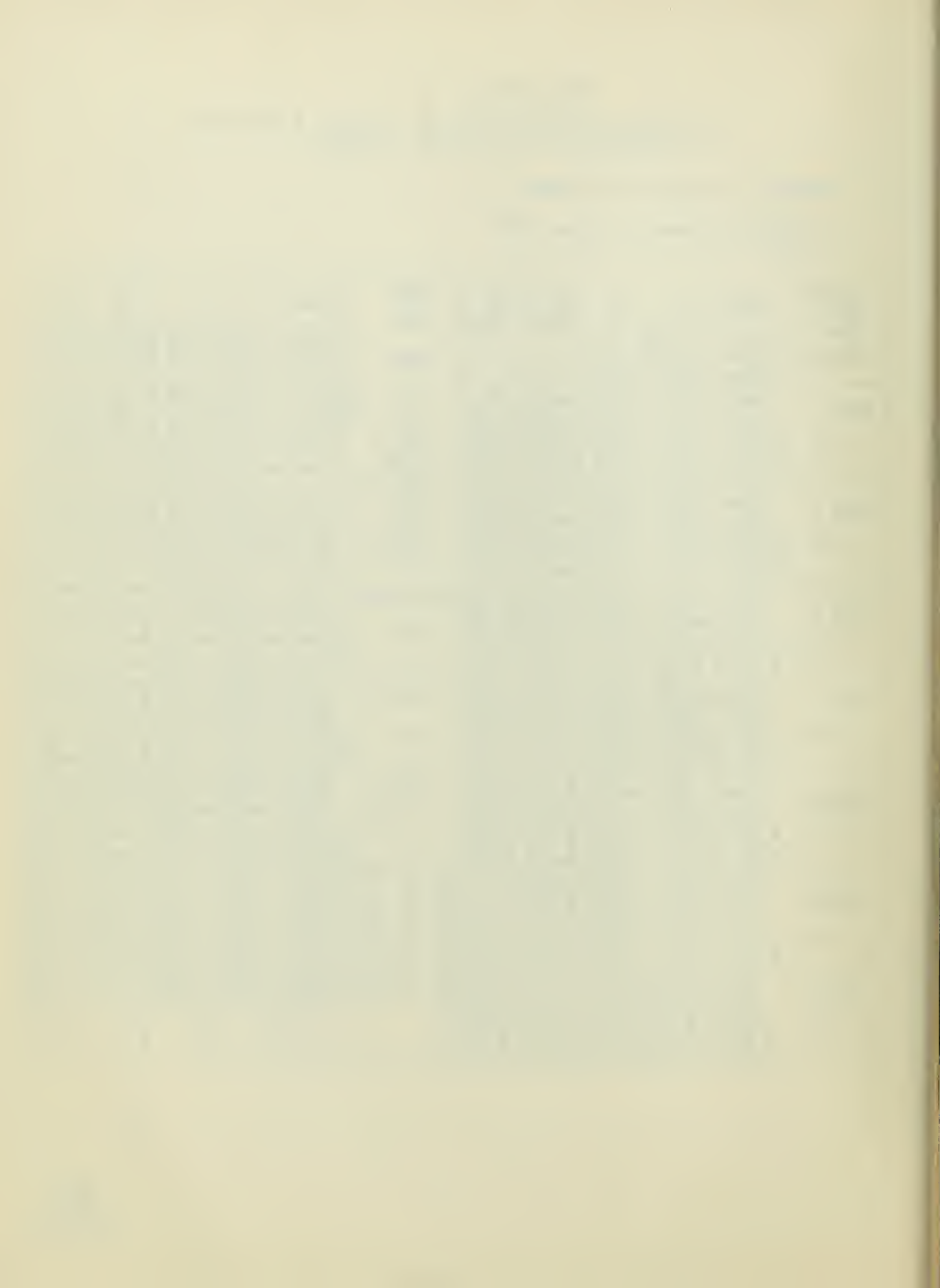
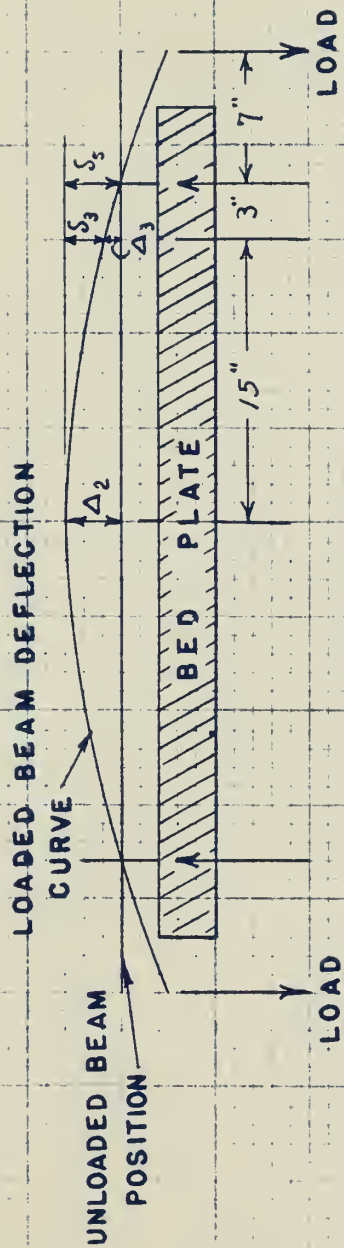


FIGURE XI
BENDING DEFLECTION
NOTATIONS



$$\delta_3 = \Delta_2 - \Delta_3$$

$$\delta_s = \Delta_2$$

8-20
L.H.L.
4-20-51



DISCUSSION OF RESULTS

The results of torsional experimentation are compared in Figure VII with the theoretical results of Chu in reference 1, which are based on the following equation:*

$$J/J_s = 1 + 2 \left[\frac{2}{15} (1 + \mu) \beta_o^2 \left(\frac{c}{h} \right)^2 \right] \quad (1)$$

Where μ = poisson's ratio, assumed .3

c = chord = 1.503"

h = thickness = .102"

J = torsional stiffness

$J_s = \frac{G}{3} c h^3$ from membrane analogy, in this case corrected for fillets.

It is readily observable that the results are comparable within limits set by the experimental limitations of the set up used in this thesis. Due to the lack of precision in measuring angles on the gauge rings the angles were measured from end to end of the entire beam. Consequently there is an indeterminent error due to the constraint of the support rings which may be noted in figures I and II. In order to bring the results more closely in line, rather complex changes would have to be made in the theory to account for fillets.

The results of the bending tests are; to the best of the author's knowledge, the first ever to be obtained, therefore there are no other

* Ref. 1, pg. 150.

The results of individual experiments are compared in Figure

VII with the theoretical results of Chu in reference 1, which are based

on the following equation:

$$(1) \quad \left[\left(\frac{c}{h} \right)^2 (1 + \mu) \left(\frac{c}{h} \right)^2 \right]^{1/2} = 1 + 2 \left[\frac{c}{h} \right]^2$$

where μ = electron's ratio, assumed 1.

c = energy = 1.505 eV

h = Planck's constant = 1.505 eV

λ = wavelength of light

$\lambda_2 = \frac{c}{h} = \frac{c}{h} \lambda$ from momentum analogy, is also

case corrected for filters.

It is readily observed that the results are comparable within

limits set by the experimental limitations of the set up used in this

series. Due to the lack of precision in measuring angles on the gage

rings the angles were measured from end to end of the entire beam.

Consequently there is an inherent error due to the constraint of

the support rings which may be noted in figures I and II. In order to

bring the results more closely in line, better support changes would

have to be made in the future to account for filters.

The results of the heading scale are to the best of the author's

knowledge, the first ever to be obtained, therefore there are no other

results or equations available for comparison. At small angles of twist below $\beta_0 = .15$ the trend of δ/δ_0 is exponential at a rate slightly less than the cube of β_0 . Above this point the curve droops, reaches a maximum of $\delta/\delta_0 = 1.32$ at $\beta_0 = .23$ and continues to the last experimental point of $\delta/\delta_0 = 1.2$ at $\beta_0 = .314$. Calculations were made as shown in Appendix C. Point 1 was not used because the slight variation in beam dimensions accentuated the error for δ_1 to an unacceptable degree. The errors inherent in the system and due to the supports, as mentioned under the torsional results; and due to lack of straightness and the consequent error if there is a slight rotation of the beam in different load conditions. It is believed that the entire beam was elastic and that the E was nearly constant during these runs, as final no-load readings checked original no-load readings for every bending test.

It was noted that the beam did not warp from the application of the permanent twist nor did the deflection rings loosen appreciably.

Despite the limited scope of these results, they show a definite loss in bending stiffness in twisted members. They are the first quantitative results to be obtained to this problem and thus are important in themselves, and as proof that further research will be rewarding.

Strain gage readings have been included in the data section of the Appendix, however, no attempt has been made to analyse them. They do, however, indicate that no permanent set took place in the beam during the bending tests. This is readily seen by obtaining the

The first of these is the fact that the average of the first 100 readings of the beam deflection was found to be 1.00 mm. This is in good agreement with the value of 1.00 mm obtained from the calibration curve. The second of these is the fact that the average of the first 100 readings of the beam deflection was found to be 1.00 mm. This is in good agreement with the value of 1.00 mm obtained from the calibration curve. The third of these is the fact that the average of the first 100 readings of the beam deflection was found to be 1.00 mm. This is in good agreement with the value of 1.00 mm obtained from the calibration curve.

strain a 3A 25 for each run, for it is noted that for each run this strain is nearly constant at 220 micro inches per inch with Ld. 2 or beam.

CONCLUSIONS AND RECOMMENDATIONS

It is concluded that the torsional results check those of Chu in reference 1, and that his equations may be used with confidence for cross sections that do not vary a great deal from simple finned forms.

The bending results show a definite loss of bending stiffness in twisted members and may be taken as the first results in a series of tests to establish workable theories for the many applications of twisted beams.

It is recommended that future tests be modified to maintain straightness and that the beam be annealed in each twisted position to assure constant E .

CONCLUSIONS AND RECOMMENDATIONS

It is concluded that the proposed results after those of Can in reference 1, and that the equations may be used with confidence for cross sections that do not vary a great deal from simple linear forms. The bending results show a definite loss of bending stiffness in twisted members and may be taken as the first results in a series of tests to establish suitable theories for the many applications of twisted members.

It is recommended that future tests be devoted to maintain straightness and that the beam be supported in each twisted position to secure constant M .

APPENDIX

APPENDIX A

Application of the Membrane Analogy.

With the beam in the initial straight condition it would be well to calculate the torsional stiffness of the beam by using the membrane analogy. This analogy establishes certain relations between the deflection surface of a uniformly loaded membrane and the distribution of stress in a twisted bar. The portion of the analogy to be used here states that twice the volume included between the surface of the deflected membrane and the plane of its outline is equal to the torque of the twisted bar.

The problem of finding the volume under the membrane that would lie over the cross section of our beam is complicated by the fillets. This cross section is shown in Figure XII. It is assumed that the membrane takes a parabolic shape. Therefore, the area A is

$$A = b^3 G \Theta / 6 \quad (2)$$

where b = width of cross section
 G = modulus of shear (11,500,000 psi)
 Θ = angle of twist in radians per inch

The problem was resolved into finding the three volumes 1, 2 and 3, and because of the symmetry of these volumes the total volume could be found. Region 1 was readily solved since b is directly known, as is the length of this straight section. In region 2 the values of b_1 , b_2 , b_3 and b_4 were found by using trigonometry and thus their parabolic areas were found. The volume of this region was then found by using Simpson's rule utilizing five equally spaced stations. The volume in region 3 was found in the same manner. However, in region 3 stations b'_2 , b'_3 and b'_4

Application of the Membrane Analogy.

With the beam in the initial straight condition it would be well to

calculate the torsional stiffness of the beam by using the membrane

analogy. This analogy establishes certain relations between the deflection

surface of a uniformly loaded membrane and the distribution of stress in

a twisted bar. The portion of the analogy to be used here states that

twice the volume included between the surface of the deflected membrane

and the plane of its outline is equal to the torque of the twisted bar.

The problem of finding the volume under the membrane that would

lie over the cross section of our beam is complicated by the ellipse.

This cross section is shown in Figure XII. It is assumed that the

membrane takes a parabolic shape. Therefore, the area A is

$$A = \frac{1}{2} G b^2 \theta \quad (2)$$

where b = width of cross section
 G = modulus of shear (11,500,000 psi)
 θ = angle of twist in radians per inch

The problem was resolved into finding the three volumes V_1 , V_2 and V_3 .

and because of the symmetry of these volumes the total volume could

be found. Region 1 was readily solved since b is directly known as is

the length of the straight section. In region 2 the values of b , θ , ϕ

and ψ were found by using trigonometry and then the parabolic area

was found. The volume of this region was then found by using Simpson's

rule utilizing five equally spaced stations. The volume in region 3 was

found in the same manner. However, in region 3 stations b_1 , θ_1 and ψ_1

do not extend to the edge of the section and the areas at these stations are made up of a rectangle beneath a parabola. The parabolic area is found by using Equation (2). The length of the base of the rectangle is known since it is the same as the base length of the parabola. The height of the rectangle is obtained from the height of the parabola at the appropriate points on station b_4 . Therefore, this height would be the mid-point height for station b_3 and the quarter point height for stations b_4 and b_2 . The quarter point heights of b_4 will be three-quarters the mid-height because of parabolic shape of the section.

Since the torque of the bar is equal to twice the volume beneath the membrane, the torque in terms of Θ follow directly. The calculated results give $\Theta = .00379$ radians/inch. From Figure VIII it is seen that for the straight beam the experimental results are 11° twist in a length of 45.1". The value of the experimental twist was then .00426 radians/inch, or 11% greater than the calculated value. This difference in results can be accounted for by the membrane not having the exact parabolic shape that was assumed and by a possible error of 3% in measuring the angle of elastic twist. With these probable errors in mind the experimental and calculated angles of elastic twist are considered to be in good agreement.

do not extend to the edge of the section and the area at these stations
are made up of a rectangle bounded by a parabola. The parabolic area is
found by using Equation (7). The length of the base of the rectangle is

known since it is the same as the base length of the parabola. The

height of the rectangle is obtained from the height of the parabola at

the appropriate points on station y_1 . Therefore, this height would be

the mid-point height for station y_1 and the quarter point height for

stations y_2 and y_3 . The quarter point heights of y_1 will be twice

quarter the mid-height because of parabolic shape of the section.

Since the top of the can is equal to twice the volume possible

the membrane, the torque intensity of θ follows directly. The calculated

results give $\theta = 0.0017$ radians/inch. From Figure VII it is seen that

for the straight beam the experimental results are 1.6° twist in a length

of 45.1". The value of the experimental twist was 0.00450 radians/inch

inch or 1.6° greater than the calculated value. This difference is

results can be accounted for by the membrane not having the exact

parabolic shape that was assumed and by a possible error of 3% in

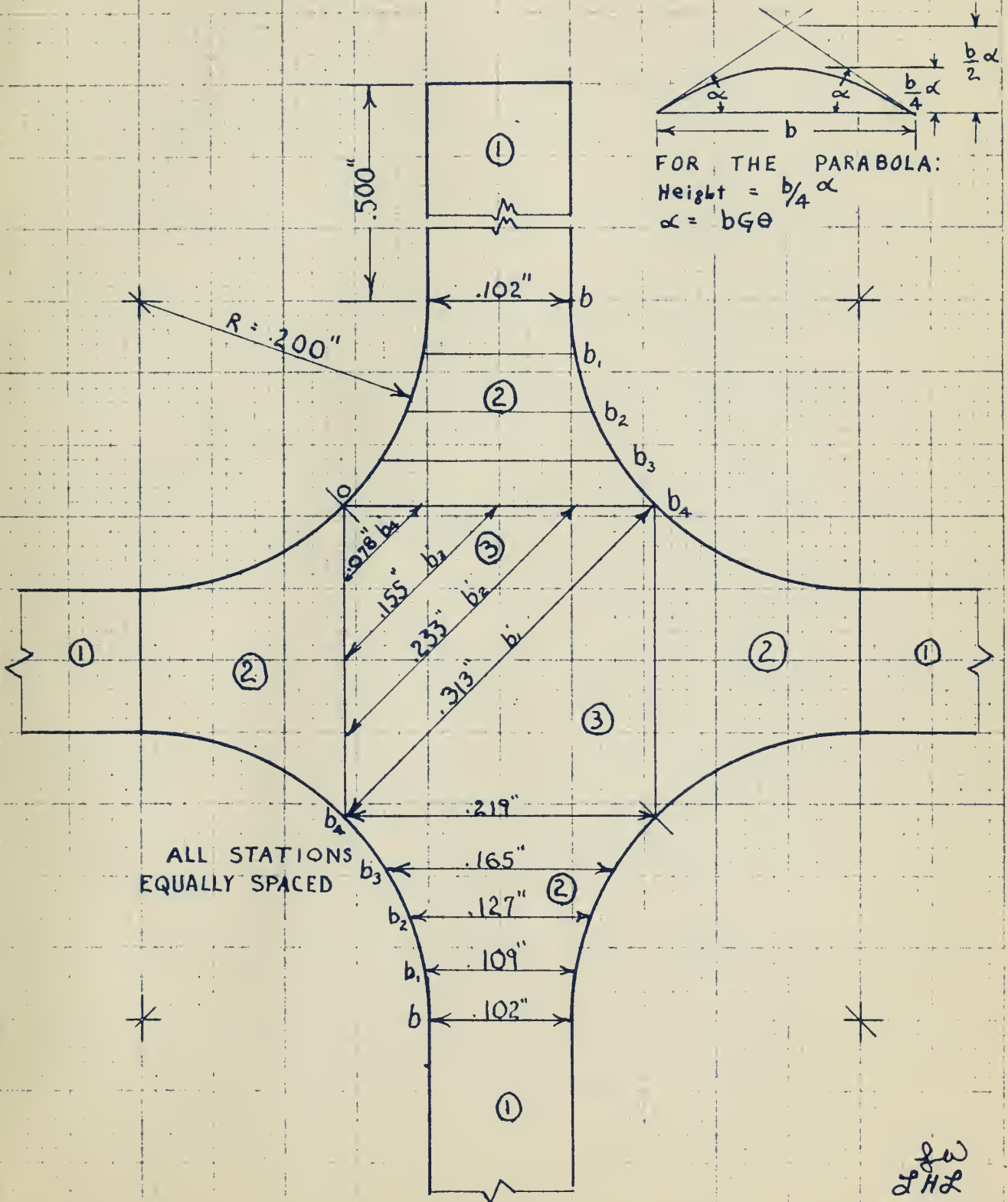
measuring the angle of elastic twist. With these probable errors in

measuring the experimental and calculated angles of elastic twist are con-

sidered to be in good agreement.

FIGURE XII

PORTION OF BEAM CROSS SECTION SHOWING STATIONS
USED IN CALCULATING MEMBRANE VOLUME USED
WITH MEMBRANE ANALOGY.



fw
LHL
4-23-51



APPENDIX B

DATA

A copy of all original data appears in Figures VIII, XIII and XIV.

APPENDIX B

DATA

A copy of all original data appears in Figures VII, VIII and XIV.

FIGURE XIII

DEFLECTION READINGS IN INCHES AT VARIOUS STATIONS, VALUES OF β_o , & VALUES OF LOAD.

NL No load on beam.

Ld.1 Load of 23.47# at each end of beam

Ld.2 Load of 45.51# at each end of beam

S indicates deflection station as shown on Figure III.

Add 1" to all readings for actual deflection above bed plate.

	THEORY		RUN 1		RUN 2		RUN 3		RUN 4		RUN 5		RUN 6		RUN 7		RUN 8	
	$\beta_o = 0$	S2	S3	$\beta_o = 0$	S2	S3	$\beta_o = .0144$	S2	S3	$\beta_o = .0257$	S2	S3	$\beta_o = .0639$	S2	S3	$\beta_o = .0807$	S2	S3
3×4																		
NL		.750	.750	.750	.751	.751	.751	.751	.753	.753	.754	.753	.755	.753	.755	.752	.756	.753
Ld.1		.781	.760	.759	.781	.760	.761	.782	.761	.784	.763	.763	.787	.763	.787	.761	.788	.763
Ld.2		.809	.769	.769	.811	.770	.810	.770	.812	.771	.813	.771	.816	.771	.817	.770	.818	.772
NL		.750	.750	.750	.751	.751	.751	.751	.753	.753	.754	.753	.755	.753	.756	.752	.756	.753
3×4																		
NL		.750	.750	.750	.751	.751	.751	.751	.753	.753	.754	.753	.754	.753	.753	.750	.754	.751
Ld.1		.781	.760	.760	.781	.760	.761	.782	.761	.784	.763	.763	.785	.763	.784	.760	.786	.761
Ld.2		.809	.769	.769	.811	.771	.812	.771	.812	.770	.814	.772	.814	.772	.813	.769	.816	.770
NL		.750	.750	.750	.751	.751	.751	.751	.753	.753	.754	.753	.754	.753	.753	.750	.754	.751

See PROCEDURE for method used in beam rotation.

3 2, 1, 4	RUN 9 $\beta_o = .1200$		RUN 10 $\beta_o = .1488$		RUN 11 $\beta_o = .1814$		RUN 12&13 $\beta_o = .227$		RUN 14 $\beta_o = .278$		RUN 15 $\beta_o = .314$		R 16 90° $\beta_o = .314$		R 18 180° $\beta_o = .314$		R 20 270° $\beta_o = .314$	
	S2	S3	S2	S3	S2	S3	S2	S3	S2	S3	S2	S3	S2	S3	S2	S3	S2	S3
NL	.760	.752	.761	.752	.765	.751	.763	.750	.760	.751	.755	.751	.750	.750	.745	.749	.750	.750
Ld. 1	.794	.763	.798	.764	.805	.764	.803	.762	.800	.764	.792	.762	.787	.762	.782	.760	.787	.761
Ld. 2	.826	.773	.833	.774	.841	.775	.840	.774	.836	.776	.827	.775	--	--	--	--	--	--
NL	.760	.752	.761	.752	.765	.751	.763	.750	.760	.751	.755	.751	.750	.750	.745	.749	.750	.750
	BEAM	ROTATED					45°		45°		45°		R 17	135°	R 19	225°	R 21	315°
NL	--	--	--	--	--	--	.755	.751	.754	.751	.753	.751	.747	.749	.747	.749	.753	.751
Ld. 1	--	--	--	--	--	--	.796	.764	.793	.763	.790	.763	.784	.761	.784	.761	.790	.763
Ld. 2	--	--	--	--	--	--	.833	.776	.829	.775	.824	.775	--	--	--	--	--	--
NL	--	--	--	--	--	--	.755	.751	.754	.751	.753	.751	.747	.749	.747	.749	.753	.751

J.H.H.
4-16-51

FIGURE XIV

STRAIN GAGE READING IN MICRO INCHES PER INCH
FOR VARIOUS VALUES OF β_0 AND FOR VARIOUS LOADS.

N.L. = No load on the beam

Ld.1 = Load of 23.47# at each end of beam.

Ld.2 = Load of 45.51# at each end of beam

STRAIN GAGE	RUN 1 $\beta_0 = 0$		RUN 2 $\beta_0 = .0042$		RUN 3 $\beta_0 = .0144$		RUN 4 $\beta_0 = .0257$		RUN 5 $\beta_0 = .0447$		RUN 6 $\beta_0 = .0639$	
	N.L.	Ld.1	N.L.	Ld.1	N.L.	Ld.1	N.L.	Ld.1	N.L.	Ld.1	N.L.	Ld.1
3A 34	5719	5820	5740	5850	5790	5890	5950	6040	6240	6330	6600	6670
3A 25	6494	6595	6445	6545	6440	6540	6470	6570	6680	6790	6940	7070
3A 20½	5360	5470	5370	5480	5400	5510	5480	5590	5700	5810	6120	6230
3A 16	6800	6895	6800	6900	6770	6870	6910	7000	7160	7270	7630	7700
4B 34	6213	6220	6240	6250	6250	6240	6250	6370	6740	6690	7070	7000
4B 25	5917	5925	5940	5950	5890	5840	5910	6000	6380	6400	6670	6690
4B 16	5910	5910	5915	5930	5990	6010	6050	6120	6430	6500	6680	6770
4B 20½	5655	5665	5675	5720			GAGE NOT GOOD					
2A 25	6810	6790	6820	6810	6790	6740	6840	6820	7040	7020	7520	7520
1B 25	6855	6735	6820	6750	6900	6780	6680	6860	7210	7090	7650	7540

STRAIN GAGE	RUN 7 $\beta_0 = .0807$		RUN 8 $\beta_0 = .1022$		RUN 9 $\beta_0 = .1200$		RUN 10 $\beta_0 = .1488$		RUN 11 $\beta_0 = .1814$		RUN 12 $\beta_0 = .227$	
	N.L.	Ld.1	N.L.	Ld.1	N.L.	Ld.1	N.L.	Ld.1	N.L.	Ld.1	N.L.	Ld.1
3A 34	7080	7130	7200	7820	8380	8370	8230	8210				
3A 25	7390	7490	7800	7920	8080	8210	9930	0050	1750	1850	GAGE NOT GOOD	
3A 20½	6670	6770	7320	7400	7940	8030	9410	9490			GAGE NOT GOOD	
3A 16	8130	8170	8600	8460	8130	8160	9130	9100	0300	0420	GAGE NOT GOOD	
4B 34	7530	7420	8280	8150	9860	9700	1160	1060			GAGE NOT GOOD	
4B 25	7180	7180	7900	7910	8390	8410	0410	0430			GAGE NOT GOOD	
4B 16	7220	7310	8000	8100	8360	8490	9940	0050			GAGE NOT GOOD	
2A 25	8060	8040	8860	8820	9330	9320	0810	0790			GAGE NOT GOOD	
1B 25	8040	7910	8910	8760	9440	9320	0820	0700			GAGE NOT GOOD	

gaw
H2
4-15-51

APPENDIX C

SAMPLE CALCULATIONS

The following calculations were made for Run 10:

$$\alpha = 567^\circ \quad L' = 50'' \quad r_0 = 0.751'' \quad \phi = 8.75^\circ$$

$$\beta_0 = \frac{\alpha \times r_0}{57.3 \times L} = \frac{567 \times .751}{57.3 \times 50} = 0.1488 \text{ rad.}$$

Torsion Calculations:

$$\theta = \frac{\phi}{57.3 \times L'} = \frac{8.75}{57.3 \times 50} = 0.00305 \text{ rad/in.}$$

$$J/J_s = \frac{.00426}{\theta} = \frac{.00426}{.00305} = 1.395$$

Bending Calculations:

	S2	S3	Δ_2	Δ_3	δ_3	δ_s
NL	1.761	1.752	---	---	---	---
Ld.1	1.798	1.764	.037	.012	.025	.037
Ld.2	1.833	1.774	.072	.022	.050	.072
NL	1.761	1.752	---	---	---	---

Δ at Ld. 1 = reading at Ld. 1 - reading at NL

$$\delta_3 = \Delta_2 - \Delta_3$$

$$\delta_s = \Delta_2$$

	$\frac{\delta_3}{\delta_{30}}$	$\frac{\delta_s}{\delta_{s0}}$
Ld. 1	$.025/.021 = 1.19$	$.037/.031 = 1.19$
Ld. 2	$.050/.040 = 1.25$	$.072/.059 = 1.22$

$$\delta/\delta_0 = \frac{1.19 + 1.19 + 1.25 + 1.22}{4} = 1.21$$

EXAMPLE CALCULATIONS

The following calculations were made for run 18:

$$\alpha = 26.7^\circ \quad L' = 20'' \quad L_0 = 0.521'' \quad \phi = 8.520^\circ$$

$$p_0 = \frac{\alpha \times L_0}{25.3 \times L'} = \frac{26.7 \times 0.521}{25.3 \times 20} = 0.1488 \text{ rad.}$$

Section Calculations:

$$\phi = \frac{\alpha}{25.3 \times L'} = \frac{26.7}{25.3 \times 20} = 0.00302 \text{ rad/in.}$$

$$1/\rho^2 = \frac{\phi}{0.00302} = \frac{0.00456}{0.00302} = 1.392$$

Bending Calculations:

WT	WT	WT	WT	Δ	Δ	Δ	Δ
1.1	1.1	1.1	1.1	1.1	1.1	1.1	1.1
1.9	1.9	1.9	1.9	1.9	1.9	1.9	1.9
1.9	1.9	1.9	1.9	1.9	1.9	1.9	1.9
1.1	1.1	1.1	1.1	1.1	1.1	1.1	1.1

Δ at 100 ft = reading at 100 ft - reading at WT

$$\Delta_2 - \Delta_1 = \Delta_3$$

$$\Delta_2 = \Delta_3$$

$$\frac{0.28}{0.28}$$

$$91.1 = 150 / 0.28$$

$$55.1 = 0.28 / 0.28$$

$$\frac{0.28}{0.28}$$

$$91.1 = 150 / 0.28$$

$$25.1 = 0.28 / 0.28$$

$$1.9.1$$

$$1.9.5$$

$$\frac{1.1 + 1.1 + 1.1 + 1.1}{4} = 1.1$$

APPENDIX D

BIBLIOGRAPHY

- (1) Chen Chu, "The Elastic Behavior of the Twisted Bourdon Tube as a Pressure Responsive Element." Sc. D. Thesis, Massachusetts Institute of Technology, 1950.
- (2) S. Timoshenko, "Strength of Materials," Vol. II, 2nd Edition, 1945.

APPENDIX B

BIBLIOGRAPHY

- (1) Chandra, "The Elastic Behavior of the Twisted Rods," *Journal of Applied Mechanics*, Vol. 1, 1934, p. 1.
- (2) S. Timoshenko, "Strength of Materials," Part I, 3rd Edition, 1955.

$$\frac{1}{\rho} = \frac{1}{\rho_0} + \frac{1}{\rho_1} + \frac{1}{\rho_2} + \dots$$

$$\frac{1}{\rho} = \frac{1}{\rho_0} + \frac{1}{\rho_1} + \frac{1}{\rho_2} + \dots$$

$\frac{1}{\rho}$	$\frac{1}{\rho_0}$	$\frac{1}{\rho_1}$	$\frac{1}{\rho_2}$	$\frac{1}{\rho_3}$	$\frac{1}{\rho_4}$	$\frac{1}{\rho_5}$
1.00	1.00	0.00	0.00	0.00	0.00	0.00
1.01	1.00	0.01	0.00	0.00	0.00	0.00
1.02	1.00	0.02	0.00	0.00	0.00	0.00
1.03	1.00	0.03	0.00	0.00	0.00	0.00
1.04	1.00	0.04	0.00	0.00	0.00	0.00
1.05	1.00	0.05	0.00	0.00	0.00	0.00
1.06	1.00	0.06	0.00	0.00	0.00	0.00
1.07	1.00	0.07	0.00	0.00	0.00	0.00
1.08	1.00	0.08	0.00	0.00	0.00	0.00
1.09	1.00	0.09	0.00	0.00	0.00	0.00
1.10	1.00	0.10	0.00	0.00	0.00	0.00

$$\frac{1}{\rho} = \frac{1}{\rho_0} + \frac{1}{\rho_1} + \frac{1}{\rho_2} + \dots$$

$$\frac{1}{\rho} = \frac{1}{\rho_0} + \frac{1}{\rho_1} + \frac{1}{\rho_2} + \dots$$

$$\frac{1}{\rho} = \frac{1}{\rho_0} + \frac{1}{\rho_1} + \frac{1}{\rho_2} + \dots$$

4 MAR 69

18132

15672

Thesis
W85

Woolston

The experimental determination of the bending and torsional stiffness of a beam with rotationally constant moment of inertia with varying amounts of permanent twist.

4 MAR 69

18132

2

Thesis
W85

Woolston

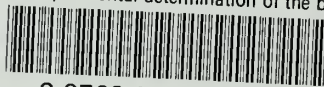
15672

The experimental determination of the bending and torsional stiffness of a beam with rotationally constant moment of inertia with varying amounts of permanent twist.

Library
U. S. Naval Postgraduate School
Monterey, California

thesW85

The experimental determination of the be



3 2768 001 90631 6

DUDLEY KNOX LIBRARY